COMPARISON BETWEEN WAVE THEORY AND ENERGY METHOD IN ACOUSTIC PREDICTION OF HVAC DUCT NETWORKS

Michihito Terao, Hidehisa Sekine and Makoto Itoh
Kanagawa university
Yokohama, 221-8686, Japan

ABSTRACT

Sound predictions based on the wave theory were carried out on HVAC duct networks. This requires the driving wave pressure amplitude and the characteristic reflection factor for every port of every component, and the complex coherence of the driving wave pressure and the characteristic transmission factor between every two of the ports of every component.
Determination techniques of these acoustic properties in the presence of airflow, and an acoustical assembly procedure of the component acoustic properties in a large-scale duct network are newly developed. Their effectiveness was confirmed by an experiment on a small-scale duct network.
Predictions by the energy base method used widely in the area were compared with those by the wave theory on HVAC duct networks for several office buildings. Consequently, it has been found that the energy base prediction easily gives about 10dB under-estimation in terms of outlet 1/3 octave band PWL.

INTRODUCTION

In HVAC duct systems, sound prediction at lower frequencies below a few hundred Hz is most important at the building space design stage, because absorbing liners are ineffective and installation of silencers of roughly a half wave length cannot be afforded after this stage.
The energy base prediction method (EGM) of ASHRAE [1] has been widely used in the area since 1940s. In this method, the sound pressure magnitudes of the connecting ducts can be determined explicitly through subtractions of the sound energy transmission-losses and additions of the generated sound energies at every component from the fan towards terminals in turn. All the contributions of the reflected waves are disregarded there. This reflection-free model makes the prediction procedure extremely simple, but reduces the reliability significantly.
In contrast, the wave base prediction method (WVM) by means of the complex sound pressures has been used to estimate the acoustic performance of reactive silencers in exhaust systems of internal combustion engines. The roles of the reflected waves are essential there, and the complex sound pressure amplitudes must be determined implicitly. Implementation of this was possible even under poor computation circumstances of several decades ago, because an exhaust system has no branches and consists of only a few acoustic components that are simply connected in series. The transverse dimensions of the pipes are small there, and the fundamental mode plane wave theory covers the important audible frequency range.
Today, even a personal computer makes it possible by means of the wave theory to predict the acoustic performance of a HVAC duct network with a few hundreds of branches. To realize the wave base prediction, component acoustic properties and procedures peculiar to this prediction must be prepared. In characterizing the active and passive acoustic properties of a component in the presence of airflow, a two-step determination method was developed. In this method the passive properties determined first and the active property determined next. To suppress undesirable flow induced microphone outputs, externally superimposed acoustic signals and additional two microphone signals are utilized for passive and active property measurements, respectively. The passive properties were determined also by numerical simulations based on a sub-region BEM (Boundary element method) and/or FEM (Finite element method).
An assembly procedure of these component properties into the combined properties in a duct network was newly developed. To confirm the effectiveness of these techniques and procedures for wave base predictions, an experimental test was conducted on a small-scale duct network. The agreement between the experiment and the prediction was excellent.
On the other hand, a HVAC duct network has rather large transverse dimensions, and the effectiveness of the fundamental mode wave theory is limited to a lower audible frequency region. The energy base method is still important for most of the audible frequency region until acoustic properties of every component become available for higher order modes. To investigate the reliability of the energy base prediction method, simulations were carried out on several realistic HVAC duct networks, and comparisons were made between the results of the energy and wave base methods.

DUCT NETWORK CONSTRUCTION

HVAC duct networks of tree-types are considered here as shown in Fig. 1. A duct network is subdivided into its components through their connecting ducts. The connecting duct must be straight and long enough to have the acoustic far field region from the discontinuities. Acoustically, it takes at least a few times of distance compared with the duct transverse dimension from the discontinuities for the evanescent waves to die out. It takes much more distance from the discontinuity for the fluid flow to reach a fully developed flow. An acoustic interface (a port) in the far field region is taken in each of the connecting duct. In order to facilitate the design iteration process and visualization of the results, an add-on computer code for automatic 3D-geometry generation of a duct network from input data was developed on a commercial PC-CAD platform with a program language.

The input data are the air quantity requirement of every outlet and the 3D geometry of the duct route by a single line representation. Fortran codes were made to automate the procedures to determine the duct sizes taking the balance of the airflow rates at each branch take-off and to determine the traveling sound pressures from each component acoustic property in a duct network.

The network topology was constructed by giving both a local port index number (defined in a component) and a global index number (defined in the network) for every port, and handled through the global port index. The output information is primarily on the round and rectangular duct size, the flow rate and airflow pressure and the traveling and local sound pressure magnitudes in every connecting duct. Interfaces from the output numerical data to several 3D graphical presentations were also made.

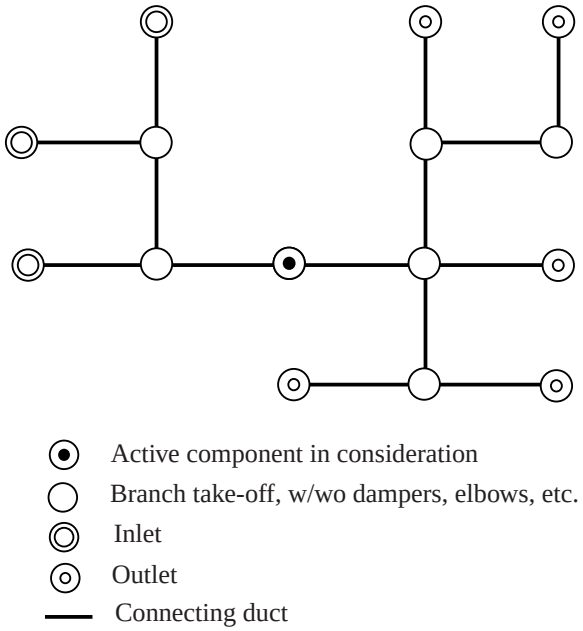

Fig. 1 A typical HVAC duct network of tree-type.

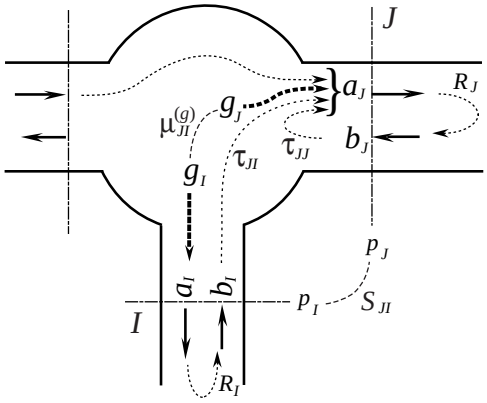

Fig. 2 Characteristic acoustic properties of a component.

ACOUSTIC EXPRESSIONS OF A DUCT COMPONENT

Acoustic properties of a component

Considering only the fundamental mode wave transmission of a single frequency here, the acoustic far field of a connecting duct can be represented by the complex pressure amplitudes of the outgoing and incoming waves a_K and b_K at every port K as shown in Fig. 2. The complex amplitude of the sound pressure p_K and the outward normal particle velocity u_K at the port can be written as

$$p_K = a_K + b_K = a_K(1+R_K)\,, \qquad (1)$$

$$u_K = (a_K - b_K)/\rho c \qquad (2)$$

where ρ is the density of air, c is the sound speed of air in still, and R_K denotes the pressure reflection factor defined as

$$R_K = b_K / a_K\ . \qquad (3)$$

For a component of M ports, applying the superposition theorem we have [3]

$$a_I = g_I + \sum_{J=1}^{M} \tau_{IJ} b_J \qquad (I = 1,2,\cdots,M) \qquad (4)$$

where the passive property τ_{IJ} denotes the characteristic transmission factor representing the contribution of b_J to a_I, as its special case τ_{II} is the characteristic reflection factor. The active property g_I denotes the driving wave pressure originated from the component going outward at its every port I. The driving wave pressure agrees with the pressure ($g_I = a_I = p_I$) at every port I, when all of the ports are anechoically terminated ($b_J = 0$ for every $J = 1,2,\cdots,M$).

By considering Eqs. (1) and (3), Eq. (4) can be written as

$$\frac{p_I}{1+R_I} = g_I + \sum_{J=1}^{M} \tau_{IJ} R_J \frac{p_J}{1+R_J}\ . \qquad (I = 1,2,\cdots,M) \qquad (5)$$

Load-combined passive properties

Eq. (4) can be rewritten as

$$g_I = \sum_{J=1}^{M} \eta_{IJ} a_J \qquad (6)$$

by employing the load-combined passive property η_{IJ} defined as

$$\eta_{IJ} = \delta_{IJ} - \tau_{IJ} R_J \qquad (7)$$

in which $\delta_{IJ} = 0$ for $I \neq J$ and $\delta_{IJ} = 1$ for $I = J$.

By using Eq. (1), Eq. (6) is rewritten as

$$g_I = \sum_{J=1}^{M} \xi_{IJ} p_J \qquad (8)$$

where

$$\xi_{IJ} = \eta_{IJ} / (1 + R_J) . \qquad (9)$$

The inverse expression of Eq. (6) is represented as

$$a_I = \sum_{J=1}^{M} \zeta_{IJ} g_J \qquad (10)$$

where ζ_{IJ} is an element of the inverse matrix $\{\zeta_{IJ}\}_{M\times M}$ of the matrix $\{\eta_{IJ}\}_{M\times M}$.

Active properties for a partially coherent source

When the pressures between the ports of an active component are partially coherent, we take the ensemble average of the cross-spectrum between pressures of every two of the ports. Taking the cross-spectrum $< g_I^* g_J > /2$ between the driving wave pressures g_I and g_J of Eq. (8), and the cross-spectrum $< a_I^* a_J > /2$ between the outgoing wave pressures a_I and a_J of Eq. (10), we have

$$< g_I^* g_J > = \sum_{L=1}^{M} \sum_{N=1}^{M} \xi_{IL} \xi_{JN} < p_L^* p_N > , \qquad (11)$$

$$< a_I^* a_J > = \sum_{L=1}^{M} \sum_{N=1}^{M} \eta_{IL} \eta_{JN} < g_L^* g_N > \qquad (12)$$

where the asterisk (*) denotes the complex conjugate, and the angle bracket (< >) denotes the ensemble average. $S_{IJ} =< p_I^* p_J > /2$ is the cross-spectrum between the pressures of every two of the ports. When $I = J$, the cross-spectra are the power-spectrum (or the mean square amplitudes) of every port I, i.e.,

$$S_{II} =< p_I^* p_I > /2 = |p_I|^2 /2 , \qquad (13)$$

$$< g_I^* g_I > /2 = |g_I|^2 /2 , \qquad (14)$$

$$< a_I^* a_I > /2 = |a_I|^2 /2 \qquad (15)$$

where the absolute symbol (| |) denotes the ensemble averaged absolute value.

The cross-spectra can be represented by means of the root mean square amplitudes and the complex coherence factors $\mu_{IJ}^{(p)}$, $\mu_{IJ}^{(g)}$ and $\mu_{IJ}^{(a)}$ between the port pressures, the driving wave pressures and the out going wave pressures, respectively, of every two of the ports I and J as

$$S_{IJ} =< p_I^* p_J > = \mu_{IJ}^{(p)} |p_I| |p_J| , \qquad (16)$$

$$< g_I^* g_J > = \mu_{IJ}^{(g)} |g_I| |g_J| , \qquad (17)$$

$$< a_I^* a_J > = \mu_{IJ}^{(a)} |a_I| |a_J| . \qquad (18)$$

DETERMINATION OF ACOUSTIC PROPERTIES OF A COMPONENT

Among the HVAC duct components, acoustic property data available to the wave theory, τ_{IJ} and g_I, are limited except the passive properties of a few basic elements such as straight ducts of acoustic far field, open ends, junctions with sudden change in cross-sectional aria, side branches, orifices and Helmholtz resonators. For most of the HVAC duct components, although approximate acoustic properties can be given by modifying existing data for extremely low frequency region, highly reliable acoustic properties must newly be prepared.

The passive property τ_{IJ} for a component is rather easily determined numerically as well as experimentally when airflow has only minor effect. However for the active property g_I caused by airflow, numerical determinations are in its beginning, and experimental determinations are still important [5-9]. For an active component such as a fan, a damper, and so on, both of the characteristic passive and active acoustic properties τ_{IJ} and g_I were determined experimentally here by applying the following two-step determination method [2,3].

Determination of passive properties

In the passive property determination, an external test signal e_N was superposed from outside of every port $N = 1,2,\cdots,M$ in turn, and the cross-spectrum between the signal e_N and p_I of Eq. (5), $S_{NI} =< e_N^* p_I > /2$, was taken in experimental measurements, i.e.,

$$\frac{< e_N^* p_I >}{1 + R_I} = \sum_{J=1}^{M} \tau_{IJ} R_J \frac{< e_N^* p_J >}{1 + R_J}$$

$$(N, I = 1,2,\cdots,M) \qquad (19)$$

where the driving wave pressure term was disregarded because the driving wave pressures are independent of the test signal.

To determine the reflection factor R_K for every port $K = 1,2,\cdots,M$, a microphone was employed at K_1 in addition to the primary microphone at every port K. The location of the primary microphone K defines the location of the port K in each of the connecting duct K. The distance ℓ_K between these microphones K and K_1 in the axial direction of every connecting duct K was taken small compared to half the shortest wavelength of interest. The reflection factor R_K was determined by using a modified version of the two-microphone method [4], i.e.,

$$R_K = \frac{S_{NK} e^{-jk\ell_K} - S_{NK_1}}{S_{NK_1} - S_{NK} e^{-jkL_K}} \tag{20}$$

where $j = \sqrt{-1}$, k denotes the wave number.

$$S_{NK} = < e_N^* p_K > / 2 \tag{21}$$

and

$$S_{NK_1} = < e_N^* p_{K_1} > / 2 \tag{22}$$

are the cross-spectrum between the test signal e_N and the microphone output p_K, and that between e_N and p_{K_1}, respectively. Undesired microphone outputs from ambient noises and the flow-induced microphone noise as well as the driving wave pressures independent of the test signal die out through those cross-spectrum measurements [11].

Eq. (19) contains $M \times M$ equations. Given S_{NK} and S_{NK_1} for every K for every N, the total $M \times M$ unknowns τ_{kj} can be determined by solving Eq. (19) simultaneously.

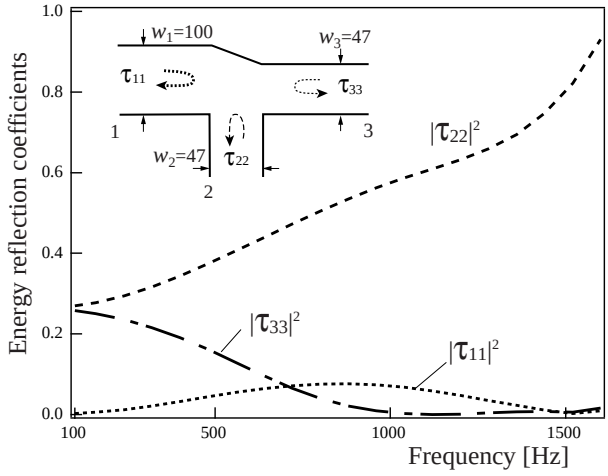

(a) Energy reflection coefficients

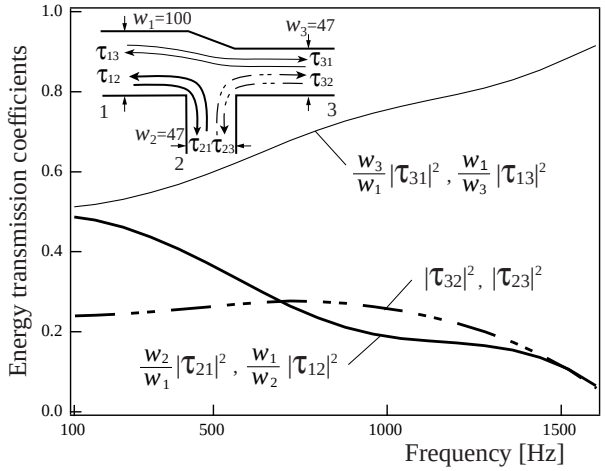

(b) Energy transmission coefficients

Fig. 3 Passive properties of a branch take off determined from BEM.

When the sound pressure distribution for every superimposed test sound e_N is given through numerical simulations, the sound pressures $p_K^{(N)}$ and $p_{K_1}^{(N)}$ for every K for every N instead of S_{NK} and S_{NK_1}, and Eq. (5) but disregarding g_I, instead of Eq. (19) can be used.

For several types and sizes of duct elbows and branch takeoffs, silencers and so on, the passive properties were determined by applying Eq. (5) and giving pressure distributions by numerical simulations based on FEM and/or BEM [12]. Fig. 3 shows the passive properties in terms of the energy transmission factors of a branch takeoff used in the subsequent simulation of a HVAC duct network.

For acoustically active components such as axial fans, centrifugal fans, volume dampers, the passive properties were determined by experimental measurements. Fig. 4(a) illustrates the semi-axial fan of domestic use applied in the subsequent simulation. Fig. 4(b) and (c) shows the acoustic passive properties of the fan under operation, determined by applying Eq. (19) and the cross-spectrum measurements. The properties are evaluated at the blade location 1 and 2 as shown in Fig. 4(a).

Determination of active properties

In this stage, removing the externally superposed test sound, every cross-spectrum S_{IJ} of Eq. (16) and every power spectrum S_{II} of Eq. (13) were measured. While the contribution of the flow induced microphone noise on each cross-spectrum S_{IJ} can be suppressed rather easily by taking large distance between every two of the ports, I and J, compared to the correlation length of turbulence, that on each power-spectrum $S_{II} = < p_I^* p_I > / 2$ can not be suppressed in this manner.

In the measurement of each power-spectrum S_{II}, an indirect measurement [3] was introduced by employing two microphones at K_3 and K_4 in addition to the primary microphone at K which defines the location of the port K in each of the connecting duct K as mentioned previously. These additional microphones K_3 and K_4, and the port microphone K were located at large distance from each other in every connecting duct K compared to the correlation length of the turbulence. The indirect measurement of every power-spectrum S_{II} uses the relationships

$$S_{II} = \frac{< p_I^* p_I >}{2} = \frac{< p_I^* p_{I_4} >< p_{I_3}^* p_I >}{2 < p_{I_3}^* p_{I_4} >}$$

$$= S_{II_4} S_{I_3 I} / S_{I_3 I_4} \tag{23}$$

where

$$S_{II_4} = < p_I^* p_{I_4} > / 2, \tag{24}$$

$$S_{I_3 I} = < p_{I_3}^* p_I > / 2, \tag{25}$$

$$S_{I_3 I_4} = < p^*_{I_3} p_{I_4} > / 2 \ , \qquad (26)$$

and nearly perfect coherence between the acoustic pressures at those microphones is assumed.

The load-combined passive properties η_{IJ} between every two of the ports I and J have been determined previously. By making the measurement of S_{II} for every port and S_{IJ} between every two of the ports, the power-spectrum $< g^*_I g_I > / 2 = |g_I|^2 / 2$ for every port and the cross-spectrum $< g^*_I g_J > / 2$ between the driving wave pressures of every two of the ports can be determined explicitly by using Eq. (11). From these power- and cross-spectra, the coherence factor $\mu^{(g)}_{IJ}$ of every two of the ports, I and J, can be given, if required, by applying Eq. (17).

The acoustic active properties of the semi-axial fan shown previously in the Fig. 4(a) were determined experimentally in this manner. For this fan [13], as shown in Fig. 4(d) and (e), the driving wave pressures towards both intake and discharge sides are, roughly speaking, similar in magnitude $|g_1| \cong |g_2|$, though partially coherent $|\mu^{(g)}_{12}| < 1$.

ASSEMBLY OF COMPONENT PROPERTIES IN A DUCT NETWORK

When the contribution of the active properties of a component to all the connecting duct pressures in a duct network is considered, this component is called active component and the other components are regarded as passive components (see Fig. 1). Every component can be an acoustically active component and contributes to the sound pressure of every connecting duct. Since the active properties of different components are independent each other, the mean squared sound pressure in every connecting duct is simply the sum of those from all of the components with active properties. The following procedure is carried out for every component with active properties in turn.

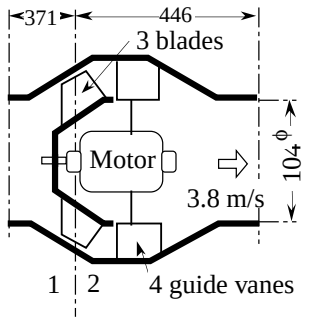

a) Semi-axial fan (2100rpm) tested.

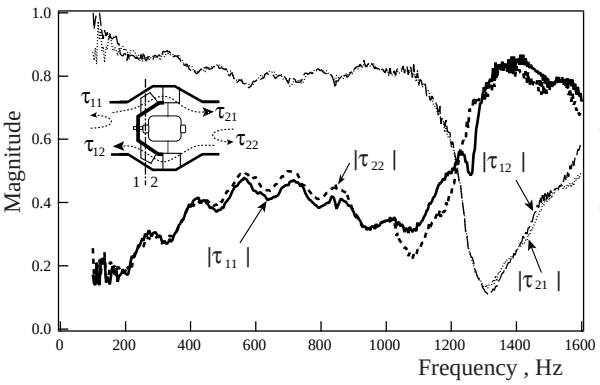

(b) Magnitude of the passive properties.

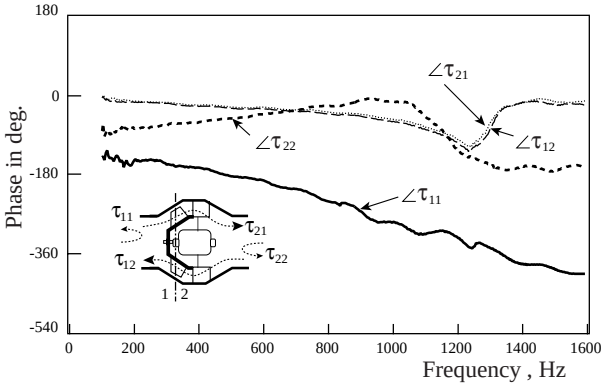

(c) Phase of the passive properties.

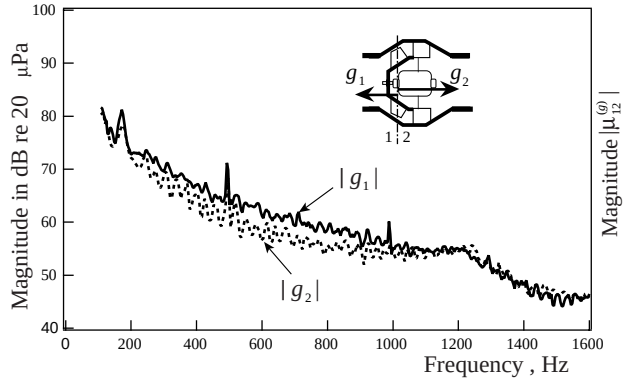

(d) Magnitude of the driving wave pressures.

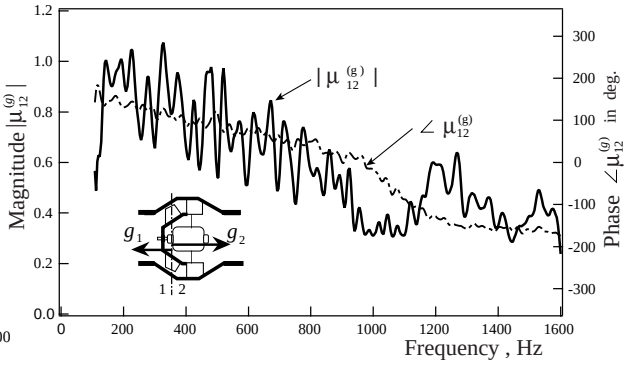

(e) Coherence between the driving wave pressures.

Fig. 4 Acoustic properties of a semi-axial fan in operation, at mean airflow velocity of 3.8 m/s.

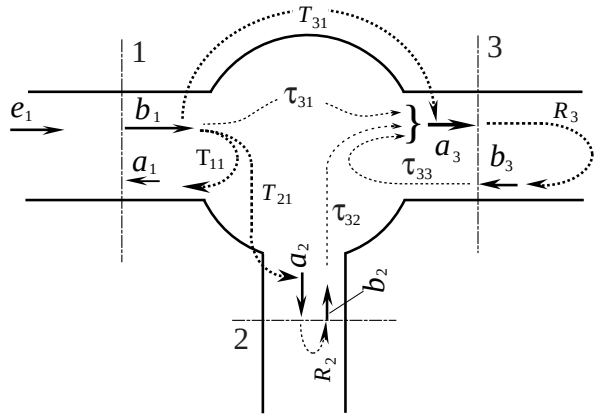

Fig. 5 Characteristic and load-combined transmission factors.

Determination of pressure transmission factors

For a passive component in a network as shown in Fig. 5, from Eq. (4) and Eq. (2) but disregarding the active property term, we have

$$T_I = \tau_{I1} + \sum_{J=2}^{M} \tau_{IJ} R_J T_J \qquad (I = 1,2,\cdots,M) \qquad (27)$$

where the port of the active component side is taken as port 1 and the pressure transmission factor T_J is defined as

$$T_J = a_J / a_1, \quad (J = 1,2,\cdots,M). \qquad (28)$$

For a passive component, from Eq. (28) and Eq. (1), we can relate the mean squared magnitudes of the outgoing wave pressure and the local sound pressure at every port to those at the port 1 as

$$|a_J|^2 = |T_J|^2 |a_1|^2, \qquad (29)$$

$$|p_J|^2 = |1 + R_J|^2 |a_J|^2. \qquad (30)$$

Given the terminal-side pressure reflection factors R_L for $L = 2,\cdots,M$, we can determine T_J for $J = 1,2,\cdots,M$ by solving Eq. (27) simultaneously. Considering the traveling wave directions defined in each component with a common port, $1/T_1$ is the load-side reflection factor of the neighboring component of the active component side. These factors of every component can be determined from every one of the terminals towards the active component in turn [14].

Determination of outgoing wave pressures of an active component

For an active component in consideration, given the load-side reflection factor R_J and the acoustic properties τ_{IJ}, the load-combined passive property η_{IJ} of every two of the ports I and J, can be obtained by applying Eq. (7). The mean squared magnitude of the outgoing wave pressure $|a_I|^2/2 = < a_I^* a_I > /2$ of every port I can be determined explicitly by applying Eq. (12) with η_{IJ} and $S_{IJ} = < g_I^* g_J > /2$ given.

Determination of outgoing wave pressures of a passive component

For every passive component from each port of the active component towards the terminals (inlets and outlets) in turn, by giving the mean square wave pressure of the active component side $|a_1|^2/2$, those of the terminal side $|a_J|^2/2$ can be determined by using Eq. (29) and the load side pressure transmission factor T_J.

Determination of outgoing wave pressures of a passive component in energy base method

A simulation by the energy base method (EGM) is simply attained by discarding all the reflection factor of every port of every component. The implicit determination process of the transmission factor T_J of Eq. (27) is not required and Eq. (27) becomes simply $T_J = \tau_{J1}$ for $J = 1,2,\cdots,M$. The outgoing wave pressure determination process of Eq. (12) also can be omitted and Eq. (12) becomes simply $|a_I|^2 = |g_I|^2$ for $I = 1,2,\cdots,M$, since $\eta_{KL} = \delta_{KL}$ for Eq. (7).

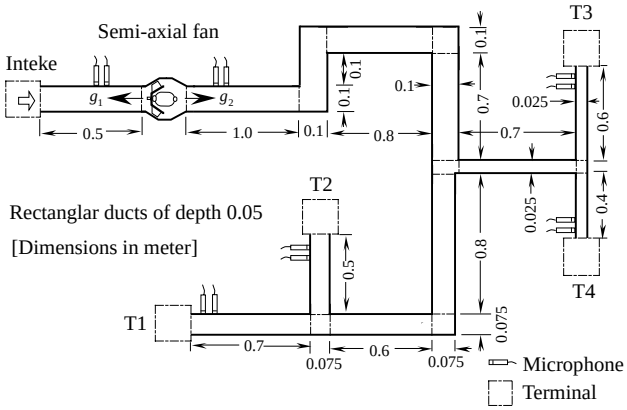

(a) Duct network tested

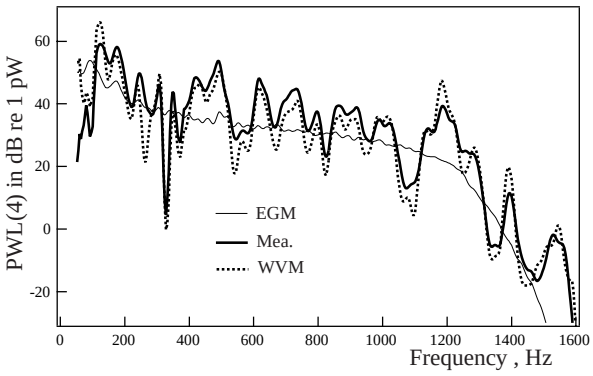

(b) PWL (4 Hz band width) of radiated sound at terminal T4.

Fig. 6 Experiment on a small scale duct network.

For every passive component from each port of the active component towards the terminals in turn, by giving the mean square wave pressure of the active component side $|a_1|^2/2$, those of the terminal side $|a_J|^2/2$ can be determined by using Eqs. (29) and the characteristic transmission factor τ_{J1} instead of T_J. For the mean square amplitude of incident wave pressure $|a_1|^2/2$ of the component directly connecting to the port K of the active component, that of the driving wave pressure $|g_K|^2/2$ of the active component is simply applied.

EXPERIMENTAL TEST OF WAVE BASE PREDICTION METHOD

The effectiveness of the introduction of the complex passive and active properties, τ_{IJ}, and $S_{IJ} = <g_I^* g_J>/2$, in sound predictions of HVAC duct networks, sound pressure calculations and experimental tests were conducted on a small scale duct network as shown in Fig. 6(a). In this network, the active component is only the semi-axial fan shown previously. The passive properties for the components other than the fan in the network were determined by means of FEM and/or BEM, disregarding stream effects. Fig. 6(b) shows a narrow band power spectrum, in terms of 4 Hz bandwidth power level, PWL(4), of the sound radiated from the terminal T4, as a typical, of the duct network of Fig. 6(a). The energy base method (EGM) gives under- and over-estimation by over 10 dB at many frequencies.

Instead, the wave base prediction method (WVM) gives excellent agreement with measurement, taking into consideration of the following phenomena. The energy loss caused by incompleteness of the duct rigidity tends to appear significantly at the resonant and anti-resonant frequencies. Ambient noises are likely to mask the radiated sound at the frequencies of low power levels in the measurement.

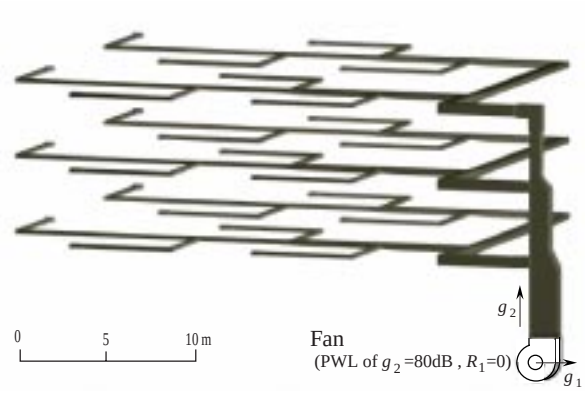

(a) A HVAC duct network used for comparison between WVM and EGM.

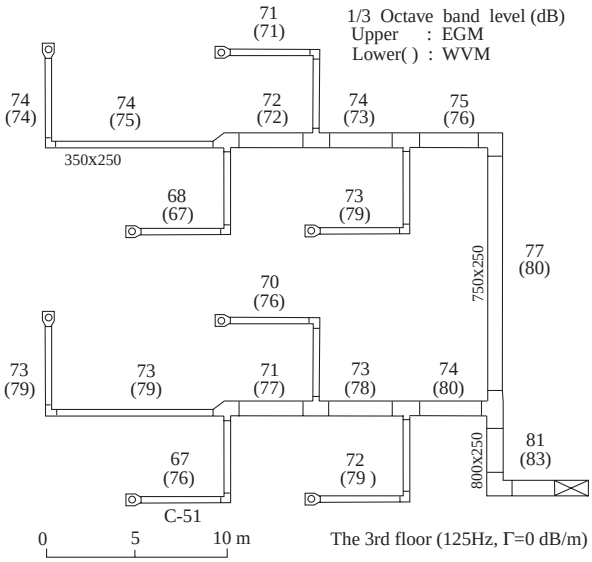

(b) 1/3 Octave-band sound pressure levels in every connecting duct of 3rd floor.

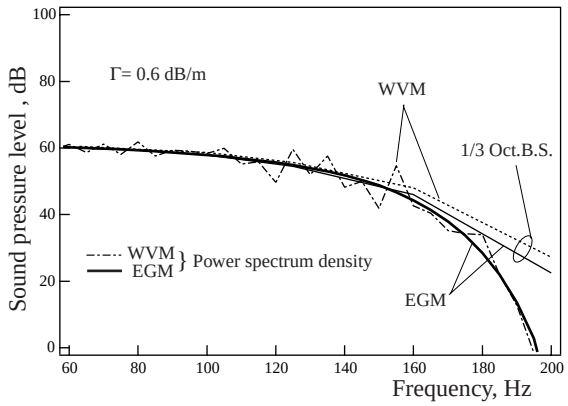

(c) Spectra in connecting duct C-51 as shown in figure (b), when Γ=0.6 dB/m.

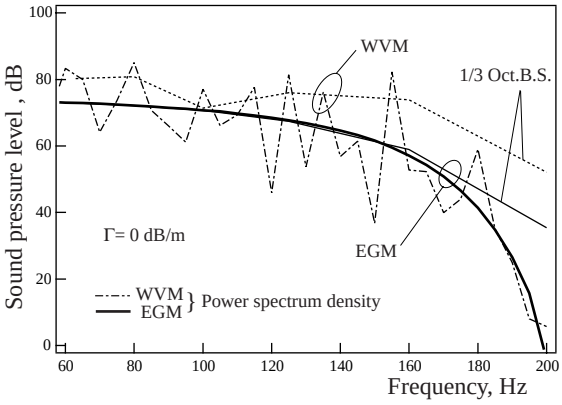

(d) Spectra in connecting duct C-51 as shown in figure (b), when Γ=0 dB/m.

Fig. 7 Comparison of outgoing wave pressure magnitudes by wave base prediction (WVM) and by energy base prediction (EGM).

COMPARISON OF ENERGY AND WAVE BASE PREDICTIONS

Simulations by energy and the wave base prediction methods were carried out, and the comparisons were made for fundamental plane wave mode on HVAC duct networks of office buildings of several stories of several floor areas as shown in Fig. 7(a). A negligibly small reflection of the intake side of the fan, $R_2 \cong 0$, was assumed here, and then only the driving wave pressure amplitude of the delivery side, $|g_1|$, is required among the acoustic properties of the fan. A power spectrum density of 80 dB at every frequency was given for $|g_1|$ in terms of the sound power level.

Fig. 7(b) shows the magnitude of the traveling wave pressure $|a_K|$ of every port K in terms of the 1/3 octave band level in each connecting duct of the network for rigid ducts (the attenuation constant $\Gamma = 0$ dB/m) at center frequency of 125Hz.

Fig.7(c) and (d) show the spectra of $|a_K|$ of the port K of a connecting duct as a typical, in terms of the spectrum density and the 1/3 octave band power spectrum for $\Gamma = 0$ and $\Gamma = 0.6$ dB/m, respectively. Since the attenuations of straight ducts Γ (dB/m) are difficult to estimate, the simulations were carried out for feasible values of Γ . When the ducts are very soft as much attenuation as $\Gamma = 0.6$ dB/m, the difference between the results of both methods is not large. It should be noted that, when the ducts are rigid, the energy base method frequently gives under-estimation by about 10 dB, even in terms of the 1/3 octave band evaluation, in the outgoing wave pressures of the connecting ducts and in the outlet sound powers.

CONCLUSIONS

Several techniques and procedures for the wave base sound prediction of a HVAC duct network were implemented. A two-step determination method was developed to obtain the amplitude and coherence of the acoustic driving wave pressure besides the characteristic reflection and transmission factor of every port of a duct component. The effectiveness of these was confirmed by an experiment on a small-scale duct network. From the sound simulations on several HVAC duct networks, it was found that the energy base method easily gives under-estimation in the outlet sound powers by about 10 dB in 1/3 octave band evaluation when the ducts are rigid.

REFERENCES

[1] ASHRAE Handbook, “Sound and vibration control”, ASHRAE Inc., USA, Applications, Chapter 43, 1995.

[2] Terao, M., Bernhard, R.J., Denton, N.L. and Sekine, H., “Sound source strength sensitivity to load impedances in an air-duct system”, Proc. INTER-NOISE 90, Gothenburg, Sweden, p591-594, Aug. 1990.

[3] Terao, M. and Sekine, H., “In-duct pressure measurements to determine sound generation, characteristic reflection and transmission factors of an air moving device in air-flow”, Proc. INTER-NOISE 89, Newport Beach, USA, p143-146, Dec. 1989.

[4] ASTM, E1050, Standard test method for impedance and absorption of acoustical materials using a tube, two microphones, and a digital frequency analysis system, 1985.

[5] Neise, W., Holste, F. and Hoppe, G., “Experimental comparison of standard sound power measurement procedures for fans”, Proc. INTER-NOISE 88, Aug. 1988, Avignon, France, p1097-1100.

[6] British Standard, “Fans for general purpose-Methods of noise testing”, British Standard Institution, BS 848, Part 2, 1985.

[7] Prasad, M.G., and Crocker, M.J., “On the measurement of internal source impedance of a multi-cylinder engine exhaust system”, J. Sound and Vibration, Vol. 90, p479-490, 1983.

[8] Munjal, M.L., and Doige, A.G., “On uniqueness, transfer and combination of acoustic sources in one-dimensional systems”, J. Sound and Vibration, Vol. 121, p25-35, 1988.

[9] Boden, H., “Characterization of fluid machines as sources of fluid borne noise”, Department of technical acoustics, Royal institute of technology, Stockholm, TRITA-TAK-8906, 1989.

[10] Terao, M. and Sekine H., “Measurement of plane wave pressures in airflow duct by the two-microphone method in a slit-tube”, Proc. INTER-NOISE 93, Aug. 1993, Leuven, Belgium, p1041-1044.

[11] Terao, M. and Sekine H., “A rejection method of the throttle noise contribution in measurement of sound generated from a HVAC duct component”, Proc. INTER-NOISE 94, Yokohama, Japan, p367-372, July 1994.

[12] Terao, M. and Sekine H., “On substructure boundary element techniques to analyze acoustic properties of air-duct components”, Proc. INTER-NOISE 87, Begin, China, p1523-1528, Sept. 1987.

[13] Terao, M., and Sekine, H., “Fan acoustical characteristics required for reliable HVAC duct sound prediction”, International INCE symposium, Fan Noise, pp343-350, Sept. 1992.

[14] Terao, M., “A method to estimate sound transmission losses in air-duct network including the contribution of reflected waves from discontinuities”, Proc. INTER-NOISE 86, Cambridge, USA, p571-576, July 1986.